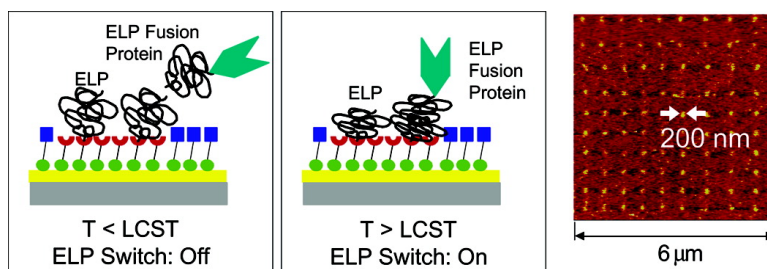


## Capture and Release of Proteins on the Nanoscale by Stimuli-Responsive Elastin-Like Polypeptide “Switches”

Jinho Hyun, Woo-Kyung Lee, Nidhi Nath, Ashutosh Chilkoti, and Stefan Zauscher

*J. Am. Chem. Soc.*, **2004**, 126 (23), 7330-7335 • DOI: 10.1021/ja049721e • Publication Date (Web): 19 May 2004

Downloaded from <http://pubs.acs.org> on March 31, 2009



### More About This Article

Additional resources and features associated with this article are available within the HTML version:

- Supporting Information
- Links to the 11 articles that cite this article, as of the time of this article download
- Access to high resolution figures
- Links to articles and content related to this article
- Copyright permission to reproduce figures and/or text from this article

[View the Full Text HTML](#)

## Capture and Release of Proteins on the Nanoscale by Stimuli-Responsive Elastin-Like Polypeptide “Switches”

Jinho Hyun,<sup>†</sup> Woo-Kyung Lee,<sup>‡</sup> Nidhi Nath,<sup>†</sup> Ashutosh Chilkoti,<sup>\*,†,§</sup> and Stefan Zauscher<sup>\*,‡,§</sup>

Contribution from the Department of Biomedical Engineering, Duke University, Durham, North Carolina 27708-0281, Department of Mechanical Engineering and Materials Science, Duke University, Durham, North Carolina 27708-0300, and Center for Biologically Inspired Materials and Materials Systems, Box 90303, Duke University, Durham, NC 27708-0303

Received January 15, 2004; E-mail: chilkoti@duke.edu; zauscher@duke.edu

**Abstract:** This article describes the fabrication and characterization of stimulus-responsive elastin-like polypeptide (ELP) nanostructures grafted onto  $\omega$ -substituted thiolates that were patterned onto gold surfaces by dip-pen nanolithography (DPN). In response to external stimuli such as changes in temperature or ionic strength, ELPs undergo a switchable and reversible, hydrophilic–hydrophobic phase transition at a lower critical solution temperature (LCST). We exploited this phase transition behavior to reversibly immobilize a thioredoxin-ELP (Trx-ELP) fusion protein onto the ELP nanopattern above the LCST. Subsequent binding of an anti-thioredoxin monoclonal antibody (anti-Trx) to the surface-captured thioredoxin showed the presentation of the immobilized protein in a sterically accessible orientation in the nanoarray. We also showed that the resulting Trx-ELP/anti-Trx complex formed above the LCST could be reversibly dissociated below the LCST. These results demonstrate the intriguing potential of ELP nanostructures as generic, reversible, biomolecular switches for on-chip capture and release of a small number (order 100–200) of protein molecules in integrated, nanoscale bioanalytical devices. We also investigated the molecular mechanism underlying this switch by measuring the height changes that accompany the binding and desorption steps and by adhesion force spectroscopy using atomic force microscopy.

### Introduction

The spatially controlled immobilization of stimuli-responsive biomacromolecules on solid surfaces at the nanometer-length scale enables fabrication of “smart”—externally switchable—protein nanoarrays with well-defined feature size, shape, and interfeature spacing. Such nanoarrays would be useful for the “on-chip” capture and release of target proteins directly from a complex mixture and would provide functionality within integrated nanoscale bioanalytical devices<sup>1–3</sup> in which the transport, separation, and detection of a small number of biomolecules must be performed in aqueous solutions.

The research presented here had two distinct objectives. The first was to use stimuli-responsive elastin-like polypeptides (ELP)<sup>4,5</sup> to fabricate a simple and generic biomolecular switch that could be implemented at the nanoscale and that would capture small numbers of protein molecules from solution and release them in response to an external trigger.<sup>6,7</sup> The second objective was to determine the molecular mechanism by which

ELPs immobilized at the surface interact with ELP fusion proteins in solution in response to external triggers.

ELPs are stimuli-responsive polypeptides<sup>4</sup> that consist of repeats of the pentapeptide sequence Val-Pro-Gly-X-Gly (VPGXG) (X is any amino acid except Pro)<sup>6,7</sup> and undergo a lower critical solution temperature (LCST) transition (commonly referred to as an inverse-phase transition within the literature pertaining to ELPs). Below their LCST, ELPs are soluble in water, but when the temperature is raised above their LCST, they undergo a sharp phase transition, leading to desolvation and aggregation of the polypeptide. Changes in the ambient temperature, ionic strength, or pH can trigger this completely reversible inverse transition.<sup>7</sup> ELPs are attractive for different applications that require molecular level control of polymer properties because they are genetically encodable and can be synthesized easily by heterologous overexpression from a synthetic gene with precise control over their composition and chain length.<sup>4,5</sup> Furthermore, the LCST of ELPs can be precisely tuned to a temperature of interest between 0 and 100 °C, which is difficult to achieve with other synthetic polymers that exhibit LCST behavior.

In previous studies,<sup>8,9</sup> we have shown that ELPs enable the fabrication of biomolecular switches using a number of different

<sup>†</sup> Department of Biomedical Engineering.

<sup>‡</sup> Department of Mechanical Engineering and Materials Science.

<sup>§</sup> Center for Biologically Inspired Materials and Materials Systems.

(1) Blawas, A. S.; Reichert, W. M. *Biomaterials* **1998**, *19*, 595–609.  
(2) Mrksich, M.; Whitesides, G. M. *Trends Biotechnol.* **1995**, *13*, 228–235.  
(3) Yu, Q.; Bauer, J. M.; Moore, J. S.; Beebe, D. J. *Appl. Phys. Lett.* **2001**, *78*, 2589–2591.  
(4) Meyer, D. E.; Chilkoti, A. *Nat. Biotechnol.* **1999**, *17*, 1112–1115.  
(5) Meyer, D. E.; Chilkoti, A. *Biomacromolecules* **2002**, *3*, 357–367.

(6) Urry, D. W.; Luan, C. H.; Parker, T. M.; Gowda, D. C.; Prasad, K. U.; Reid, M. C.; Safavy, A. *J. Am. Chem. Soc.* **1991**, *113*, 4346–4348.  
(7) Urry, D. W. *J. Phys. Chem. B* **1997**, *101*, 11007–11028.

designs.<sup>10</sup> In one implementation of a “smart”, switchable interface, an ELP was patterned on a surface at the microscale, and the micropatterned, stimuli-responsive ELP features were shown to reversibly capture ELP fusion proteins from a complex mixture.<sup>9</sup> Directly motivated by these previous studies, our objective in this study was to fabricate a *nanoscale biomolecular switch on a surface* using stimuli-responsive ELP components for the reversible, “on-chip” capture and release of a few hundred molecules.

The nanoscale biomolecular switch in this study had two components: first, a genetically engineered stimuli-responsive ELP that was end-grafted to carboxyl-terminated, self-assembled monolayers (SAMs) nanopatterned onto a gold surface by dip-pen nanolithography (DPN),<sup>11–13</sup> and second, a recombinant ELP fusion protein<sup>4,14</sup> that had the same ELP appended on its C-terminus as that immobilized on the surface. To create the surface-bound component of the biomolecular switch and to demonstrate proof-of-principle of nanoscale, on-chip separation, and release of proteins, we fabricated ELP nanoarrays with feature sizes as small as 200 nm by DPN. We chose DPN as the fabrication methodology for several reasons. First, DPN is inexpensive and convenient, in that it does not require a clean room environment and can be carried out using widely available AFM instrumentation. Second, DPN is a simple nanopatterning method that enables rapid prototyping of nanostructures, without extensive lead time.

In this article, we show that the two components of the biomolecular switch can be reversibly associated and dissociated on a surface at the nanoscale by simultaneously triggering the inverse phase transition of the surface-bound ELP and of a thio-redoxin-ELP fusion protein (Trx-ELP) in solution. We demonstrate the functional utility of this nanoscale switch by reversibly immobilizing a small number (order 100–200) of ELP fusion proteins onto each nanoscale feature of the ELP array. We furthermore show that the immobilized ELP fusion proteins can bind a Trx-specific antibody and that the bound complex of the Trx-ELP and antibody can be quantitatively desorbed from the surface upon reversing the LCST transition of the ELP, resulting in the regeneration of the surface back to the ELP array. Force spectroscopy provided, for the first time, direct measurements of conformational and surface energetic changes that accompanied the collapse of end-grafted ELP in response to the LCST transition. These measurements suggest that hydrophobic interactions between the ELP on the surface and its ELP fusion protein partner in solution are responsible for their association above the LCST.

These studies are the first, we believe, to demonstrate the capture and release of a small number of biomolecules in response to an external trigger on nanopatterned surfaces. This study thereby provides proof-of-principle that effective capture, presentation, and release of biomolecules can be achieved and monitored “on-chip” in a planar architecture at the nanoscale and provides a molecular mechanism for the “on-chip” nanoscale biomolecular switch.

## Experimental Section

**Elastin-Like Polypeptides.** The ELP used in this study consisted of 180 pentapeptide repeats, with a total molecular weight of 71.9 kDa. It contained Val, Ala, and Gly at the guest residue positions of the pentapeptide, in a 5:2:3 ratio, respectively. We used the overexpression of a plasmid-borne synthetic gene in *Escherichia coli* to synthesize the ELP and a Trx-ELP fusion protein, in which the same ELP was fused to the C-terminus of Trx (MW ~14 000 g/mol).<sup>4,5,14</sup> In brief, cells harboring a plasmid that encodes for either the ELP, Trx-ELP, or Trx (control) were grown in 50 mL of CircleGrow culture media (Bio101, CA) supplemented with 100  $\mu$ g/mL ampicillin, with shaking at 300 rpm at 37 °C. Cell growth was monitored by the optical density (OD) at 600 nm (OD<sub>600</sub>), and the addition of isopropyl  $\beta$ -thiogalactopyranoside (IPTG) to a final concentration of 1 mM induced protein expression at an OD<sub>600</sub> of 1.0. After incubation for 3 h at 37 °C, the cells were recovered from the culture medium by centrifugation (2500g, 4 °C, 15 min) and resuspended in 5 mL of phosphate-buffered saline solution (PBS, 140 mM NaCl, and 2.7 mM KCl). The cells were lysed by sonication and centrifuged at 16000g for 20 min, and the supernatant containing the ELP or Trx-ELP was collected for purification. The ELP and the Trx-ELP fusion protein were purified by inverse transition cycling, as described elsewhere.<sup>14</sup>

**Gold Substrates.** We prepared gold substrates with an average Au grain diameter of 30 nm on glass cover slides by thermal evaporation of a chromium adhesion layer (10 nm), followed by gold (100 nm), at a pressure of  $4 \times 10^{-7}$  Torr. Before deposition, the glass surface was cleaned for 20 min in a 5:1:1 (v:v) mixture of H<sub>2</sub>O, H<sub>2</sub>O<sub>2</sub>, and NH<sub>4</sub>OH at 80 °C.

**Nanopatterning.** Using DPN,<sup>11–13</sup> we patterned 16-mercaptohexadecanoic acid (MHA, Sigma-Aldrich) using an atomic force microscope (AFM) (MultiMode, Veeco Digital Instruments).<sup>15</sup> To charge an AFM cantilever tip (NanoProbe,  $k \approx 60$  pN/nm, Veeco Digital Instruments) with thiol “ink”, the lever was incubated for 1 min in a saturated solution of MHA in degassed acetonitrile. Patterns of MHA on gold were generated with writing speeds up to 8  $\mu$ m/s; the relative humidity during patterning ranged from 35 to 55%. Video images of patterned surfaces with registration marks were recorded during DPN to enable subsequent pattern localization. Unpatterned regions on the gold substrate were passivated by incubation in a 1 mM solution of 11-mercaptoundecyltri(ethylene glycol) (EG<sub>3</sub>-SH) in ethanol for 1 h and subsequently rinsed with ethanol for 10 min. The formation of an EG<sub>3</sub>-terminated alkanethiol SAM on regions of the gold substrate that were not patterned with MHA by DPN minimizes nonspecific protein adsorption in subsequent processing steps.

**ELP Immobilization.** The COOH groups in the MHA SAM were reacted with *N*-hydroxysuccinimide (NHS) (0.2 M, Aldrich) and 1-ethyl-3-(dimethylamino)propyl carbodiimide (EDAC) (0.1 M, Aldrich) in Milli-Q grade water for 30 min. The samples were sonicated in ethanol for 5 min, rinsed with ethanol and Milli-Q grade water, and dried in a stream of N<sub>2</sub> gas. Next, a 200  $\mu$ L droplet of a 1.6  $\mu$ M solution of the ELP in PBS was pipetted onto the patterned area and left for 10 min to covalently conjugate the ELP to the surface. The substrate was washed with a 0.05% sodium dodecyl sulfate (SDS, Pierce) solution to desorb unreacted ELP from the surface, and then exhaustively rinsed with PBS and Milli-Q grade water. We immediately imaged the surfaces using TappingMode AFM in liquid to visualize the ELP nanostructures.

**Inverse Transition Cycling.** To reversibly capture Trx-ELP, we incubated an ELP nanopattern for 10 min with 1.6  $\mu$ M solution of Trx-ELP in PBS containing an additional 1.5 M NaCl (PBS and 1.5 M NaCl). After incubation, the substrate was rinsed with PBS and 1.5 M NaCl and imaged using TappingMode AFM in the same buffer to

(8) Frey, W.; Meyer, D. E.; Chilkoti, A. *Langmuir* **2003**, *19*, 1641–1653.  
(9) Nath, N.; Chilkoti, A. *Anal. Chem.* **2003**, *75*, 709–715.  
(10) Nath, N.; Chilkoti, A. *Adv. Mater.* **2002**, *14*, 1243–1247.  
(11) Hang, S. H.; Mirkin, C. A. *Science* **2000**, *288*, 1808–1811.  
(12) Hong, S. H.; Zhu, J.; Mirkin, C. A. *Science* **1999**, *286*, 523–525.  
(13) Piner, R. D.; Zhu, J.; Xu, F.; Hong, S. H.; Mirkin, C. A. *Science* **1999**, *283*, 661–663.

(14) Meyer, D. E.; Trabbic-Carlson, K.; Chilkoti, A. *Biotechnol. Prog.* **2001**, *17*, 720–728.  
(15) Hyun, J.; Ahn, S. J.; Lee, W. K.; Chilkoti, A.; Zauscher, S. *Nano Lett.* **2002**, *2*, 1203–1207.

confirm the binding of Trx-ELP to ELP nanopatterns. The surface was subsequently rinsed for 10 min with PBS at 4 °C to release the captured Trx-ELP fusion protein and imaged by TappingMode AFM in PBS and 1.5 M NaCl to verify desorption of the fusion protein by measuring the heights of the patterned features. Imaging in PBS and 1.5 M NaCl kept the ELP on the surface in a collapsed state and hence helped to maintain a consistent ELP pattern height for comparison. In a separate set of experiments that were designed to test the functional presentation of the captured Trx-ELP fusion protein, Trx-ELP was bound to the ELP nanopatterns by incubation from solution as previously described, and the surface was then immediately incubated with 25 nM anti-Trx monoclonal antibody (MBL International Corp.) in PBS and 1.5 M NaCl for 5 min at room temperature. The surface was then imaged by TappingMode AFM in PBS and 1.5 M NaCl. After AFM imaging, the Trx-ELP/anti-Trx complex was desorbed by a 10 min exposure to PBS at 4 °C and imaged by AFM again in PBS and 1.5 M NaCl. In a control experiment that was designed to test whether Trx alone would bind to ELP above the LCST, we used TappingMode AFM to image the ELP nanopattern immediately after it had been incubated for 10 min with 1.6  $\mu$ M Trx in PBS and 1.5 M NaCl and then gently washed with PBS and 1.5 M NaCl.

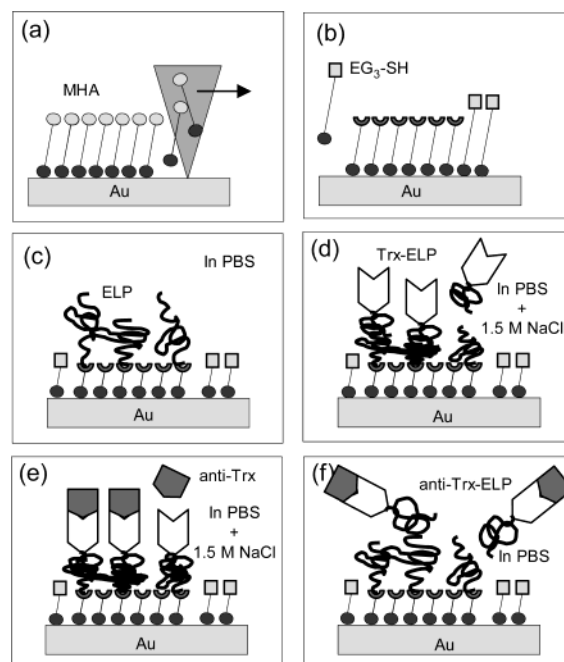
**Surface Force Measurements.** We used AFM in force spectrometry mode (Veeco, Digital Instruments MultiMode AFM with Nanoscope IIIa controller) to measure interaction forces between an ELP-coated gold surface and a cantilever tip that was also covalently functionalized with an ELP. The ELPs were covalently attached onto flat gold substrates and onto gold-coated AFM tips using the procedure for ELP attachment described above. Cantilever spring constants were estimated from the power spectral density of the thermal noise fluctuations.<sup>16</sup> The typically observed RMS noise of force was about 20 pN, in good agreement with the estimated thermal force fluctuations of 18 pN. The sensitivity of the photosensitive detector was determined from force-separation plots, using the constant compliance regime upon approach at large applied normal force. The zero of separation was customarily chosen to coincide with the constant compliance regime. For force measurements, the sample and the cantilever were subjected to the same medium conditions as for the inverse transition cycling experiments, described above.

## Results and Discussion

**Nanopatterning.** Nanopatterning of ELP involves several steps that are outlined in Scheme 1. First, MHA is patterned by DPN on a thermally evaporated gold surface (Scheme 1a). Second, the surface is incubated with EG<sub>3</sub>-SH to form a protein-resistant “nonfouling” SAM in the nonpatterned region of the substrate; the terminal COOH groups on the patterned MHA SAM are then activated with NHS and EDAC (Scheme 1b).<sup>17,18</sup> Third, ELPs are immobilized by reacting their amine groups with activated carboxyl groups on the surface (Scheme 1c). ELP has only two amine groups, one of which is the N-terminal amine and the other is on the side chain of the sole lysine residue present in the ELP, located at the third position in the amino acid sequence. Hence, we believe that ELP is end-grafted at the surface in a highly oriented fashion.

This methodology routinely generated ELP patterns having a lateral feature size of about 200 nm. The lateral feature size of an ELP pattern typically matched that of the underlying MHA template to within 5 nm, indicating that the feature size of the MHA template governs the lateral feature size of an ELP pattern. We also found that the minimum achievable lateral feature size depended significantly on the surface roughness of the underly-

Scheme 1<sup>a</sup>



<sup>a</sup> (a) DPN of MHA. (b) Backfilling with EG<sub>3</sub>-SH and activation of MHA. (c) End-grafting of ELP. (d) Immobilization of Trx-ELP fusion protein to an ELP pattern above the LCST. (e) Specific binding of anti-Trx mAb to Trx-ELP above the LCST. (f) Release of fusion protein complex from ELP pattern below the LCST. (MHA = mercaptohexadecanoic acid; Au = gold; ELP = elastin-like polypeptide; EG<sub>3</sub>-SH = 11-mercaptoundecyltri(ethylene glycol); Trx = Thioredoxin; anti-Trx = Thioredoxin antibody.)

ing gold layer. The passivation of the unpatterned background with EG<sub>3</sub>-SH SAMs was critical in preventing nonspecific protein adsorption to the surface and in turn yields a high signal-to-noise ratio for binding assays.

**Inverse Transition Cycling.** Thermodynamically reversible LCST transitions of ELPs are most commonly triggered either by temperature changes or, isothermally, by changes in the type and concentration of salts.<sup>19</sup> For experimental convenience, we opted for the latter and added NaCl to trigger the LCST transition of the ELP in solution and on the surface. The feature height of ELP on surfaces depends on the molecular size and conformational state of the ELP. ELP conformation is a function of the grafting density and solvent quality and is affected by the AFM imaging conditions, particularly the applied imaging force. When imaged by AFM in TappingMode, the average feature height of surface-grafted ELP was between 5 and 6 nm in PBS and about 3 nm in PBS and 1.5 M NaCl, using imaging forces on the order of a few hundred piconewtons. These feature sizes for end-grafted ELPs are consistent with steric interaction distances obtained from force spectroscopy measurements at forces of about 150–200 pN (see Figure 3c below). Our AFM height measurements suggest that the addition of 1.5 M NaCl to PBS triggers the phase transition of surface-immobilized ELPs.

**Capture of ELP Fusion Proteins.** To demonstrate the functional utility of the reversibly switchable interfacial phase transition behavior of ELPs, we captured an ELP fusion protein (Trx-ELP) from solution onto an end-grafted ELP nanopattern. To achieve this, we simultaneously triggered the LCST of the

(16) Hutter, J. L.; Bechhoefer, J. *Rev. Sci. Instrum.* **1993**, *64*, 1868–1873.

(17) Lee, K. B.; Park, S. J.; Mirkin, C. A.; Smith, J. C.; Mrksich, M. *Science* **2002**, *295*, 1702–1705.

(18) Prime, K. L.; Whitesides, G. M. *Science* **1991**, *252*, 1164–1167.

(19) Kontturi, K.; Mafé, S.; Manzanares, J. A.; Svarfvar, B. L.; Viinikka, P. *Macromolecules* **1996**, *29*, 5740–5746.



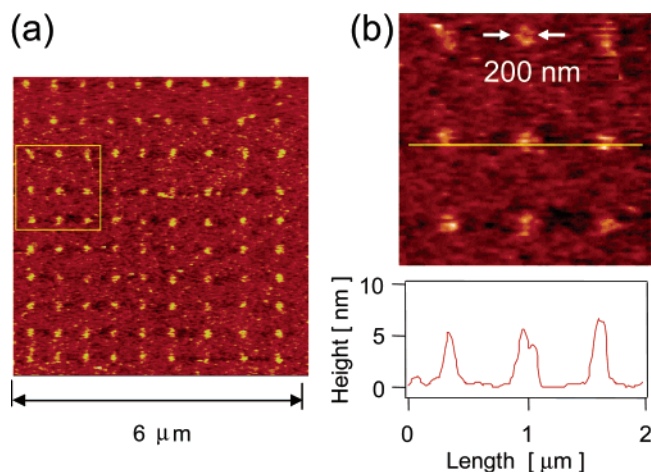


**Figure 1.** (a) AFM TappingMode height image of a  $10 \times 9$  ELP dot array in PBS buffer at room temperature. (b) Enlarged view of area indicated in (a) and representative cross section, showing a typical feature height of 5 to 6 nm and a lateral feature size of about 200 nm.

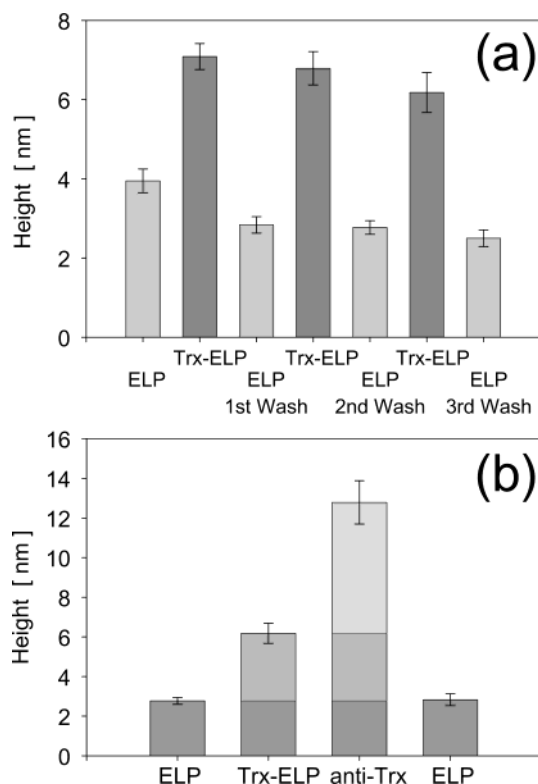


**Figure 2.** Reversible immobilization of Trx-ELP fusion protein onto an ELP array by isothermally shifting the LCST through changing the salt concentration in PBS buffer at room temperature. (a) Average feature heights for three repeated adsorption-wash cycles. (b) Average feature heights after incubation with Trx-ELP and anti-Trx mAb, and after washing in PBS. Average feature heights were obtained in all cases from AFM TappingMode height images in PBS with 1.5 M NaCl added.

immobilized ELP on the surface and the Trx-ELP in solution by adding 1.5 M NaCl to the buffer. In PBS, an additional 1.5 M NaCl depresses the LCST of the ELP below the ambient temperature, so that the immobilized ELP on the surface and the Trx-ELP in solution undergo their LCST transition simultaneously (Scheme 1d).<sup>10,20</sup> After incubation with Trx-ELP, the height of the nanostructures in the array increased by about 3.5 nm. This height increase is reasonable considering that the fusion protein, in which the Trx moiety constitutes about 16% of the

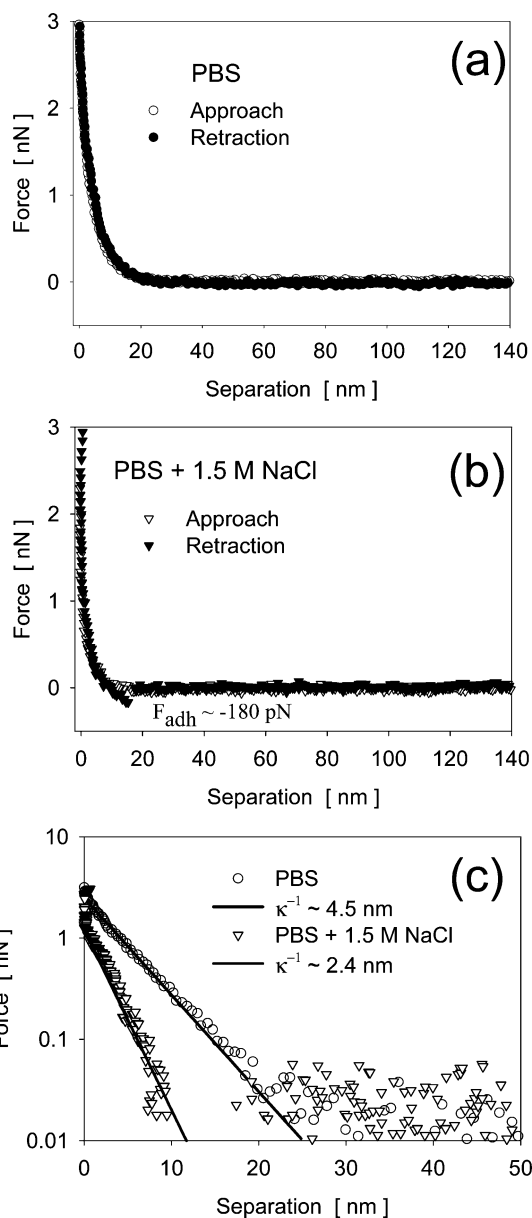


**Figure 3.** Surface force measurements between two ELP-decorated surfaces using AFM. Typical force response plotted as a function of separation (a) below and (b) above the LCST, showing the presence of an adhesive force upon separation above the LCST. Insets: Schematic illustration of the measurement configuration and the solvent-dependent ELP conformation below and above the LCST. (c) Force upon approach plotted on a logarithmic scale as a function of separation below and above the LCST, showing the decrease in steric interaction above the LCST.

total molecular mass, has a somewhat larger molecular size than the ELP alone. After incubation in PBS, which shifts the LCST to above room temperature and thereby reverses the phase transition, the Trx-ELP was released from the ELP pattern. Figure 2a shows that the average feature height of an ELP pattern (again imaged in PBS and 1.5 M NaCl) decreased to about 3 nm after the first transition cycle. This is somewhat smaller than the original height of the ELP pattern and indicates desorption of the bound Trx-ELP fusion protein. This conformational change was reversible through many cycles of the LCST transition. However, the pattern height decreased slightly with each desorption step (Figure 2a), indicating that either some

(20) Frey, W.; Meyer, D. E.; Chilkoti, A. *Adv. Mater.* **2003**, *15*, 248–251.

of the surface-immobilized ELP molecules were lost or that a small fraction of the surface-immobilized ELP underwent an irreversible conformational collapse upon repeated cycling through the LCST transition. To test whether Trx alone would bind to surface-immobilized ELP above the LCST, we incubated an ELP nanopattern with Trx in PBS and 1.5 M NaCl. These control experiments showed no statistically significant difference in feature height before and after incubation, suggesting that Trx alone does not bind to surface-immobilized ELP.

These results suggest that significant binding of an ELP fusion protein to the nanopatterned ELP occurs only when both the ELP fusion protein in solution and the immobilized ELP on the surface simultaneously undergo their LCST transition. The LCST transition leads to hydrophobic interactions between the surface-immobilized ELP and the ELP tail of individual fusion protein molecules. The reversible height increase of about 3.5 nm observed by AFM is consistent with binding of individual molecules of Trx-ELP to surface-immobilized ELP. These results rule out two other potential mechanisms by which an ELP fusion protein can interact with the surface. First, the measured feature heights were too small for aggregates of the ELP fusion proteins that are formed in solution as a consequence of the LCST transition of Trx-ELP to have interacted with the desolvated ELP on the surface above the LCST. Second, the measured feature heights are also too small to account for heterogeneous nucleation of aggregates of Trx-ELP on sites provided by defects in the ELP monolayer at the surface, as was shown to occur for the interaction of Trx-ELP with a CH<sub>3</sub>-terminated alkanethiol SAM on gold above the LCST of the fusion protein.<sup>8</sup>

We estimate an upper bound for the number of ELP fusion protein molecules immobilized on an ELP nanostructure with a diameter of 200 nm to be on the order of about 200 molecules. This estimate is obtained by simply dividing the area of the patterned feature by the area that one fusion protein covers above the LCST. In this calculation, we assumed that the diameter of the area occupied by an ELP fusion protein immobilized on the ELP surface is about twice the radius of gyration of a surface-immobilized ELP molecule above its LCST and, furthermore, that the ELP fusion proteins are close-packed on the surface. Surface force measurements yielded a value of 7 nm for the radius of gyration for a surface-immobilized ELP above its LCST (see below). The actual number of molecules immobilized is most likely less than 200, considering that a Trx-ELP fusion protein is larger than an ELP alone and that close packing of Trx-ELP on the nanoscale features of the ELP surface is unlikely.

The ELP array with Trx-ELP immobilized above the LCST was next incubated with anti-Trx to demonstrate the functional presentation of the immobilized Trx-ELP. AFM measurements showed that the pattern height increased by about 6.5 nm (Scheme 1e, Figure 2b). This was likely due to the molecular recognition-mediated binding between the immobilized Trx and its antibody, and it suggests that the Trx moiety of Trx-ELP was preferentially oriented outward from the patterned surface. The complex of Trx-ELP and anti-Trx could be released from the ELP nanopattern by increasing the LCST to above room temperature by incubation in cold PBS (Scheme 1f, Figure 2b).

**Surface Force Measurements.** Previous studies, which exploited the optical transduction of the LCST transition by gold nanoparticles, provided only an indirect measure of the con-

formational and energetic changes associated with the LCST transition of surface-bound ELPs at the molecular scale.<sup>21</sup> We performed AFM surface force measurements on surface-immobilized ELP below and above the LCST to directly probe the molecular mechanism of this interaction. The insets to Figure 3a,b illustrate schematically the measurement configuration and the solvent-dependent ELP conformations. When two ELP-decorated surfaces are brought into increasingly compressive contact, repulsive steric forces arise from the restriction of conformational degrees of freedom in the thermally mobile polypeptide chains. Since experiments were performed in PBS buffer and in some instances with large amounts of salt added (further shielding electrostatic interactions), repulsive force contributions due to electric double layer overlap were small and short ranged (decay lengths are less than 1 nm). The separation distance,  $D$ , between the sample surface and the cantilever tip was calculated by letting the constant compliance region, the region at which the stiffness of the compressed sample exceeds the spring constant of the cantilever, coincide with  $D = 0$ . This means that  $D$  could be in error up to twice the thickness of a highly compressed ELP molecule. However, this error in  $D$  is likely small, considering the enormous pressure exerted by the AFM cantilever tip on the ELP sample in the constant compliance regime.

Figure 3a shows that the interaction upon approach and retraction was monotonically repulsive in PBS (i.e., solution conditions in which the ELP is below its LCST) and that the onset of steric interactions occurred at a separation ( $D$ ) of about 25 nm. This thickness corresponds to an ELP height of about 12 nm on each of the two surfaces and agrees with the estimated radius of gyration ( $R_g \approx 14$  nm) of an end-grafted ELP with 180 pentapeptide repeats. The  $R_g$  of an ELP immobilized on a surface at low grafting densities was estimated assuming that the ELP is a flexible polymer chain with a Flory characteristic ratio of 10 in an athermal solvent.<sup>22</sup> These assumptions are justified by MD simulations that indicate ELP below the LCST behaves as a thermally mobile, flexible biomacromolecule.<sup>23</sup>

In PBS with 1.5 M NaCl added, the surface-immobilized ELP undergoes its LCST transition, and the force upon approach goes through a small attractive minimum before becoming monotonically repulsive at a separation of about 15 nm (Figure 3b). This corresponds to an ELP height of about 7 nm on each of the two surfaces. The force minimum likely arises from attractive hydrophobic segment–segment interactions whose magnitude increases with increasing compression until, with further compression, the restrictions in conformational degrees of freedom finally dominate and give rise to strong, steric-repulsive forces. The force-separation profiles upon approach plotted in Figure 3c clearly show the conformational collapse of ELP caused by the LCST transition. This collapse can be quantified by the decrease in decay length ( $\kappa^{-1}$ ) from 4.5 nm in the extended state below the LCST to 2.4 nm above the LCST. This is obtained by fitting an inverse exponential function,  $F(D) \propto e^{-\kappa D}$ , to the data where  $F$  is the force and  $D$  is the separation distance. The ELP feature heights that are obtained from the force measurements by halving the distances at which the onset of steric interaction occurs are significantly larger than the ELP

(21) Nath, N.; Chilkoti, A. *J. Am. Chem. Soc.* **2001**, *123*, 8197–8202.

(22) Rubinstein, M.; Colby, R. H. *Polymer Physics*; Oxford University Press: Oxford, New York, 2003.

(23) Li, B.; Alonso, D. O. V.; Daggett, V. *J. Mol. Biol.* **2001**, *305*, 581–592.

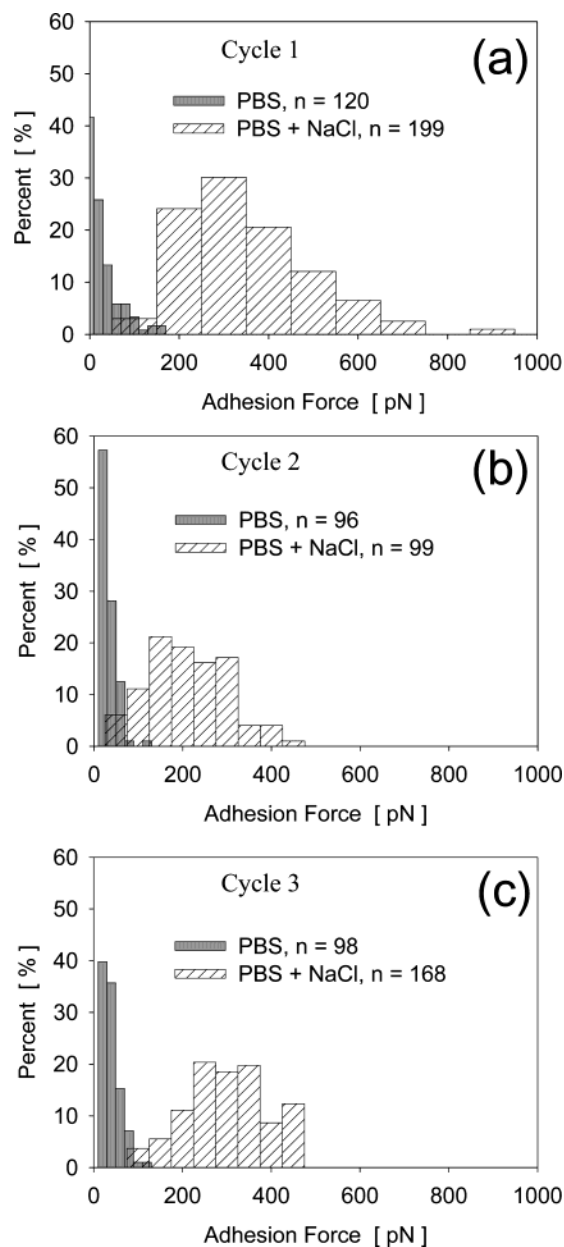


**Figure 4.** Adhesion forces between two ELP-decorated surfaces in PBS for three transition cycles where the LCST is switched isothermally by addition of 1.5 M NaCl to PBS. Adhesion forces after the (a) first, (b) second, and (c) third inverse transition cycle, showing that significant adhesion forces only occur above the LCST (in the presence of 1.5 M NaCl).

heights obtained from AFM TappingMode height images (Figures 1 and 2). This discrepancy is resolved when considering that the ELP is noticeably compressed at the tapping forces ( $\sim 200$  pN) used in AFM TappingMode imaging.

We hypothesized that the reversible immobilization of an ELP fusion protein on an ELP pattern is caused by the reversible change in surface energy associated with the LCST phase transition. To test this hypothesis, we measured the maximum force (i.e., the pull-off force) required to liberate an ELP-decorated cantilever from an ELP-covered surface, below and above the LCST (Figure 3a,b). The pull-off force is a good measure of adhesion, and thus surface energy, as it does not contain contributions from elastic surface deformation. Figure 4 shows that significant adhesion forces between ELPs exist only above the LCST and that below the LCST the adhesive interactions are

small and on the order of the force uncertainty introduced by the thermal noise fluctuations of the cantilever. The reversibility of these adhesion forces was demonstrated by cycling the ELP isothermally through its LCST transition with the addition of 1.5 M NaCl to the PBS buffer and by subsequently reversing the LCST transition by replacing the high salt buffer in the AFM fluid cell with PBS. Nearly identical distributions of the pull-off force were obtained in each of the three LCST cycles, suggesting that the effect of the LCST transition on adhesion and surface energy is entirely reversible (Figure 4a–c).

## Summary and Conclusions

In summary, we have demonstrated the fabrication of stimulus-responsive elastin-like polypeptide nanostructures that were covalently end-grafted onto  $\omega$ -substituted thiolates; the thiolates were in turn patterned onto gold surfaces by dip-pen nanolithography. We exploited the hydrophilic–hydrophobic phase transition of ELP in response to a change in ionic strength as a switch to reversibly immobilize a thioredoxin-ELP fusion protein onto the ELP nanopattern above the lower critical solution temperature. We demonstrated the biological activity of the Trx-ELP nanoarray by binding an anti-thioredoxin monoclonal antibody. Furthermore, we showed that the resulting Trx-ELP/anti Trx-mAb complex could be released below the LCST.

Our results demonstrate proof-of-principle that “smart”, surface-confined biomolecular switches can be built at the nanoscale. The two components of the switch are activated in response to external triggers, such as changes in the temperature or ionic strength of the solvent. This method of fabricating switchable surfaces is attractive because it is entirely modular and generic, in that it only requires an ELP-modified or patterned surface and a protein that can be appended with an ELP tag. ELP synthesis is easily achieved through genetic engineering techniques. Furthermore, we demonstrate in this article the functional utility of the biomolecular surface switch to reversibly capture an ELP fusion protein from solution. Within a 200 nm pad of immobilized ELP, a small number ( $\sim 100$ – $200$ ) of the Trx-ELP fusion protein molecules can be captured, presented, and released reversibly from the surface in response to an external trigger. The nanoscale miniaturization of on-chip separation and the presentation and triggered release of the captured proteins made possible by this methodology should be integrable into nanoscale bioanalytical devices that are currently under development.

**Acknowledgment.** We thank Professor Buddy Ratner (University of Washington, Seattle) for the generous gift of the EG<sub>3</sub>-thiol and Professor Elizabeth Paley (Duke University) for valuable feedback on the manuscript. This work was partially supported by a grant from the National Institutes of Health to A.C. (GM023632) and by the National Science Foundation through a grant to S.Z. (DMR-0239769 Career Award). A.C. and S.Z. would also like to thank the National Science Foundation for support through Grant NSF EEC-021059.

JA049721E